Bulletin of the New Zealand Society for Earthquake Engineering, Vol. 51, No. 1, March 2018

CYCLIC RESPONSE ANALYSIS OF HIGH-STRENGTH SELF-COMPACTING CONCRETE BEAM-COLUMN JOINTS: NUMERICAL MODELLING AND EXPERIMENTAL VALIDATION

Mohammad Soleymani Ashtiani[1], Rajesh P. Dhakal[2] and Allan N. Scott[3]

(Submitted *November 2016*; Reviewed *January 2017*; Accepted *February 2017*)

ABSTRACT

In this paper, finite element analysis software "DIANA" is implemented to simulate quasi-static cyclic loading test results of three full-scale beam-column joints cast with high-strength self-compacting concrete (HSSCC). The specimens were designed according to the New Zealand concrete standard (NZS3101 2006). Material models for concrete and steel were calibrated based on the physical characteristics of the materials derived either from laboratory tests or using expressions available in literature. Two-dimensional curved-shell elements were used in modelling the specimens. As the specimens were designed following the code requirements for seismic actions, bond between the reinforcement and concrete was assumed as perfect. In order to obtain a more representative prediction, both the longitudinal and transverse reinforcement were modelled in their actual locations. Pushover analyses were first conducted to check the mesh sensitivity; after which the modelled specimens were subjected to reversed cyclic loading histories applied in the experimental tests. Seismically important response parameters such as damping, stiffness, concrete and steel contributions in the joint shear resistance, joint shear deformation, strain development in the joint stirrups, elongation of the plastic hinge zone, development of compressive stress, and cracking pattern were extracted from the analytical predictions and compared to the experimental results. It was found that the adopted modelling and analysis approach was capable of predicting cyclic performance of HSSCC beam-column subassemblies with reasonable accuracy.

INTRODUCTION

Reinforced concrete (RC) beam-column joints (BCJ) behave in a very complex manner when subjected to cyclic actions. In general, a RC BCJ may exhibit a combination of different failure mechanisms such as diagonal joint shear failure, flexural hinging of beam triggered by yielding of reinforcement, and excessive bond slip resulting in loss of anchorage of beam longitudinal bars. Therefore, any analytical model aiming to reliably predict the joint behaviour should be capable of capturing these failure mechanisms and other unique characteristics contributing to the joint response.

Finite element analysis (FEA) of BCJs accounting for such behaviours has been the focus of many previous research studies. Some researchers have tried to model the nonlinear behaviour of beam-column joints by manually updating the material properties at the onset of cracks or through the specification of discrete cracks [1]. However, difficulty in pre-specifying crack locations motivated researchers to adopt continuum-based elasto-plastic fracture models. Amongst the most commonly used models are the Drucker-Prager plasticity model paired with a multidirectional non-orthogonal fixed crack model, the micro-plane models, the Willam-Warnke plasticity model in conjunction with a smeared rotating crack model, and the smeared rotating crack model along with the Modified Compression Field Theory (MCFT). Explanation of the details of these analytical models is out of the scope of this paper and can be found in literature [1].

This paper presents an analytical model developed to predict the cyclic performance of high-strength self-compacting concrete (HSSCC) beam-column joints. So far, various micro analyses [2,3] have been performed to assess/predict the seismic performance of conventionally vibrated BCJs of normal/medium strength concrete (of compressive strength between 30 and 70 MPa). When dealing with HSSCC, the high-strength material properties as well as the differences in the mix proportion may affect the mechanical properties (such as modulus of elasticity and bond) in comparison to the normal concrete. Therefore, there is a need to scrutinize the suitability of the available concrete models and analytical procedures in capturing the behaviour of HSSCC BCJs under cyclic loading. The significance of this research lies in providing analytical evidence in predicting seismic performance of HSSCC BCJs through concrete and reinforcement material models originally developed for conventionally vibrated concrete of normal strength (with calibration if/as needed).

For the numerical investigations reported in this study, a finite element analysis program DIANA [4] was chosen as it is known to be capable of convincingly dealing with the complexities and nonlinearities involved in modelling reinforced concrete. It was chosen not only because of its reported success in simulating highly nonlinear problems [1,2,5,6], but also because it has multiple constitutive models for concrete and steel to choose from. Three experimentally tested HSSCC beam-column subassemblies were modelled and analysed using DIANA. The available material models for steel and concrete were calibrated to suit the behaviour of HSSCC and the reinforcing bars used

[1] *Corresponding Author, Structural Engineer, Connor Consulting Ltd, Christchurch, NZ, ms.ashtiani81@gmail.com*

[2] *Professor, Department of Civil and Natural Resources Engineering, University of Canterbury, Christchurch, NZ, rajesh.dhakal@canterbury.ac.nz (Fellow)*

[3] *Senior Lecturer, Department of Civil and Natural Resources Engineering, University of Canterbury, Christchurch, allan.scott@canterbury.ac.nz (Member).*

in the tested specimen. Nonlinear pushover and cyclic analyses were performed on the modelled specimens and seismically important features predicted by the analysis were compared with the experimental results.

MATERIAL MODELS

Total strain rotating crack model, which is based on the MCFT [7] and follows a smeared crack approach [8], was used to model the constitutive behaviour of concrete. The implemented formulation in DIANA includes three-dimensional extension of the MCFT theory proposed by Selby et al. [9,10], which accounts for lateral expansion and changes in concrete strength due to confinement and/or transverse cracking. The total strain crack model describes stress as a function of strain. As currently implemented in DIANA, the loading is modelled differently under tension and compression; however the unloading follows a secant path back to the origin (Figure 1).

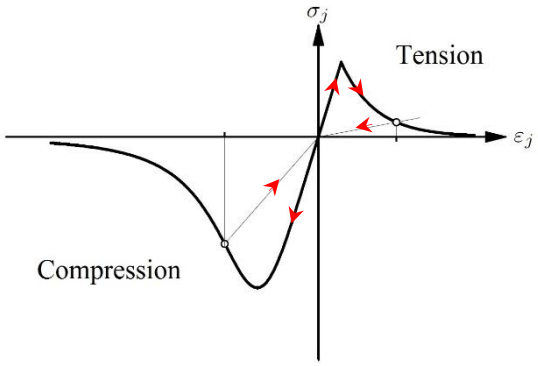

Figure 1: Total strain crack model loading/unloading paths.

In the 'rotating crack model' the crack direction is allowed to continuously adjust itself to the direction of principal compressive strain. Although this approach bears less physical meaning than the 'fixed crack model' (where crack direction remains the same after its occurrence), it has been successfully applied to simulate the behaviour of RC structures for a long time. A rotating crack model is advantageous over a fixed crack model in shear-failure type problems because the specification and validation of a shear retention factor is not required. However, the assumption that the principal stresses and strains remain coincident is considered a limitation of this approach.

The concrete constitutive response consists of uniaxial tensile and compressive stress-strain envelopes as detailed below. During loading, concrete is subjected to either tensile or compressive stress which can result in cracking or crushing. Deterioration of concrete due to cracking and crushing is monitored with internal damage variables which track the maximum (tensile) and minimum (compressive) strains reached at each integration point. In the total strain rotating crack model, it is assumed that once the material (concrete in this case) is damaged, it will not recover. Therefore, the absolute values of the internal damage variables and thus the stiffness degradation can only increase.

The lateral deformations of a specimen subjected to uniaxial tensile or compressive loadings are governed by the Poisson effect. However, a passive lateral confinement emerges when these displacements are constrained, which is an important characteristic in a three-dimensional modelling of RC structures. When the material is cracked, the Poisson effect is no longer valid. This means that expansion in the cracked direction will not result in contraction of the transverse direction. As concrete is a pressure-dependent material, confinement plays an important role in changing its strength and ductility. Compressive behaviour is also affected by lateral cracking, or in other words by its tensile strength deterioration in the transverse direction.

The concrete constitutive model detailed above depends on the selection of uniaxial concrete tensile and compressive behaviours. This means that the total strain rotating crack model may be coupled with various choices of tension and compression curves to simulate the concrete behaviour. The compression and tension envelopes of the concrete model were adopted from Thorenfeldt et al. [11] and Hordijk [12], respectively. The monotonic envelopes and the cyclic loops used in the compression and tension domain of the concrete constitutive models are schematically shown in Figure 2. Note that the stress-strain envelope shown in Figure 2 is originally developed for conventionally vibrated normal strength concrete, which is used mainly to emphasize the shapes of the envelopes and the origin-targeted unloading and reloading loops. As is well-known, high strength will make the concrete response more brittle, but the stress-strain envelopes of conventional and self-compacting concrete are believed to be similar. As can be seen in the figure, the adopted cyclic model does not account for the residual strain and the unloading/reloading loops always pass through the origin with secant stiffness. Although this reduces the accuracy of the FEA in predicting cyclic response of concrete, the overall flexural response of RC members is governed by the constitutive model of reinforcement.

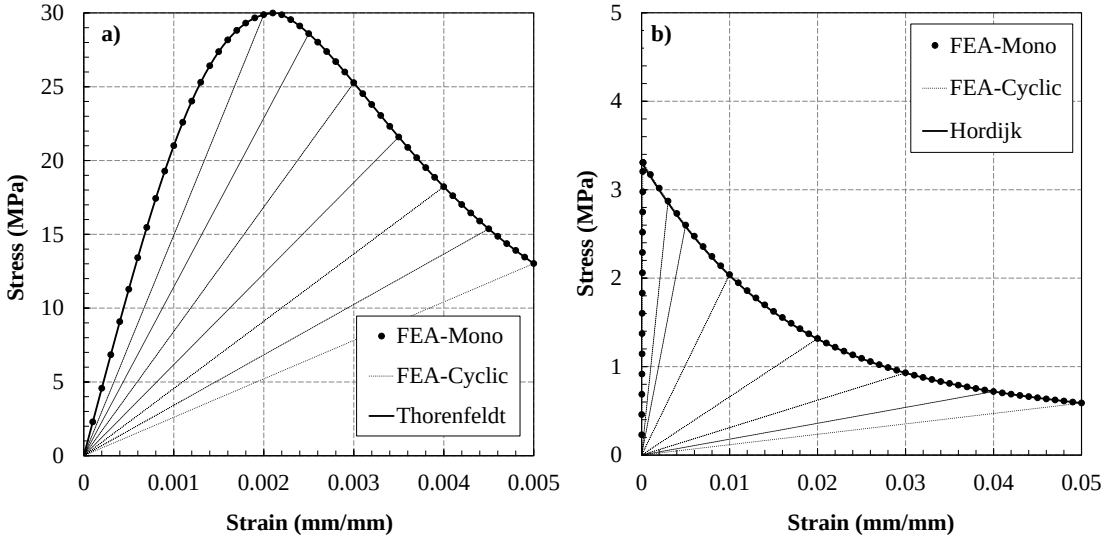

Figure 2: Stress-strain envelopes and the cyclic loops adopted in the model for concrete in (a) Compression [11]; (b) Tension [12].

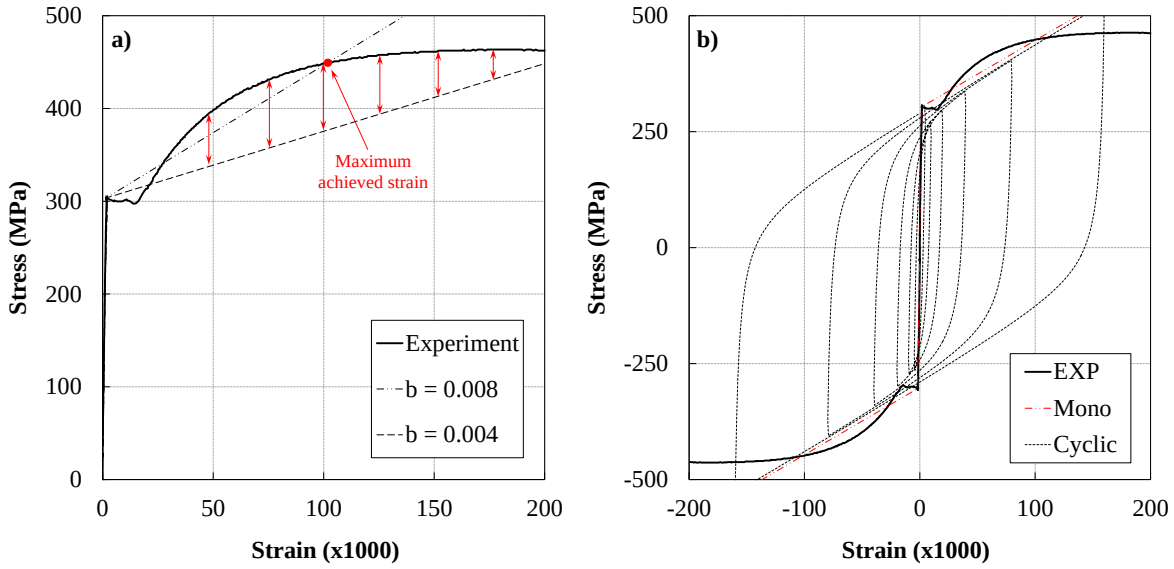

Figure 3: Menegotto-Pinto model for monotonic and cyclic stress-strain response of steel bars.

Cyclic performance of RC BCJs is highly dependent on the nonlinear response of steel bars under cyclic loading. One of the important features of the nonlinear behaviour of reinforcing steel under cyclic excitations is its behaviour during loading reversal; more commonly known as the Bauschinger effect. Many researchers have successfully investigated the Bauschinger effect in the behaviour of reinforcing steel [13-18]. Some have also accounted for buckling effect in rebar models [19-24]. The effect of rebar unloading/reloading loops on the predicted performance of cyclically loaded joints has been scrutinized previously [25,26]; and it was found to affect the performance of compression zone.

In this study, the constitutive response of steel was modelled using Menegotto and Pinto model [13] coupled with a bilinear backbone curve. The detailed formulation of the model can be found in many previous studies [1,13]. Parameters of the Menegotto-Pinto model were set based on a parametric analysis and recommendations from literature [1,13,27] i.e. R_0 = 19.5, A_1 = 18.5, A_2 = 0.1, A_3 = 0.0, and A_4 = 0.0. In order to determine an appropriate value for the strain hardening ratio 'b', experimental stress-strain curves for the reinforcement were used. Figure 3a shows the experimental response of a typical D25 bar under axial tension. The Menegotto-Pinto model follows a bilinear curve in which the first branch connects the origin and the yielding point so that the elastic behaviour of the reinforcement can be predicted accurately. The ratio of strain hardening 'b' should be calculated in such a way that the second branch fits the post-yield phase of the steel response. The first choice is to determine 'b' so that the second branch of the model connects the yielding point to the maximum strain before failure (b = 0.004 line in Figure 3a). However the problem with this way of determining 'b' is that the model constantly underestimates the response of reinforcement after yielding by upto about 20%, which is a substantial compromise in one of the main material models.

Therefore, a more realistic approach was chosen to determine the ratio of strain hardening which is detailed herein. It is known that the maximum elongation of the reinforcement takes place in the plastic hinge zone. As a result, the maximum strain that the reinforcement had undergone at the end of the test was used to determine the stress from the experimental stress-strain curves for reinforcement. The achieved point was connected to the yield point and the slope of this line provided a more realistic value for the strain hardening ratio (b = 0.008) which was used in the Menegotto-Pinto model. Figure 3a shows the comparison of the two (b = 0.004 and 0.008) values chosen for the strain hardening ratio. After the steel strain reaches a value of 0.1 mm/mm, the model (incorporating b=0.008) starts overestimating the stress-strain response. However, as mentioned before the maximum measured strain in the steel was well below 0.1 mm/mm. Thus, it is expected that a 'b' value of 0.008 well serves the purpose of FEA modelling of the specimens used in this study; especially given that a multilinear backbone model is not available in DIANA to be used with Menegotto-Pinto model [13]. Figure 3b compares the Menegotto-Pinto model for both monotonic and cyclic loads with a typical experimental monotonic stress-strain curve. It is clear that the cyclic response of the model, accounts for plastic strain; therefore, the overall member response should be able to capture plastic deformations due to the yielding of steel.

Reinforcing steel can be modelled using three different options in DIANA; namely embedded reinforcement, discrete reinforcement and bond-slip reinforcement. Employing discrete reinforcement elements and connecting them to concrete using interface elements (such as bond-slip) is advantageous only when a detailed bond-slip analysis is required. However in most of the other cases (such as BCJs), embedded reinforcement is normally used which can be coupled with the bond-slip option if necessary (such as for non-seismically detailed BCJs where slipping of the beam bars through the joint might happen). Depending on the distribution of reinforcement over the RC section, either 'bar' or 'grid' reinforcement option can be utilized. Note that in the 'bar' reinforcement option, although the embedded reinforcement is used, the bars can be defined at their exact locations.

The bond between reinforcement and concrete was modelled using a perfect-bond assumption for two reasons. First, as the BCJs were designed to satisfy the seismic requirements of the current NZ concrete standard [28], slip of bars through the joint is not considered a probable failure mechanism. Second, in the current version of DIANA [4] the bond-slip for embedded reinforcement has not been coupled with the Menegotto-Pinto model [13]. Therefore, if the bond-slip has to be used, the Menegotto-Pinto model should be replaced with the Von Mises Plasticity model for reinforcement. However, the latter was found to overestimate the energy dissipation in each stress-strain loop. As the importance of the steel model is more critical than the effect of bond-slip behaviour for seismically detailed BCJs, it was decided to forego the complex bond-slip implementation in the finite element modelling.

DEVELOPMENT OF THE FINITE ELEMENT MODEL

The BCJ specimens chosen for FEA were part of a bigger scale research project on seismic performance of HSSCC in RC structures. They were fabricated using commercially reproducible HSSCC mix [29]. The specimens comprised of a 5 m long beam and a 2.9 m tall column. The beam and column had cross sections of 340 x 420 mm and 340 x 520 mm, respectively. Grade 300 MPa and 500 MPa steel were used in different specimens for the longitudinal and transverse reinforcement. The subassemblies were instrumented with load cells, potentiometers and strain gauges in order to capture the required information necessary for the calculation of seismically important features. The specimens were tested under a fully reversed cyclic loading regime up to 4.5% drift under different axial loads (namely 200 kN and 1500 kN). Details of the mix designs, specimens, testing procedure, and experimental results as well as other relevant information are presented elsewhere [30,31]. The test setup used to test the specimens is shown in Figure 4.

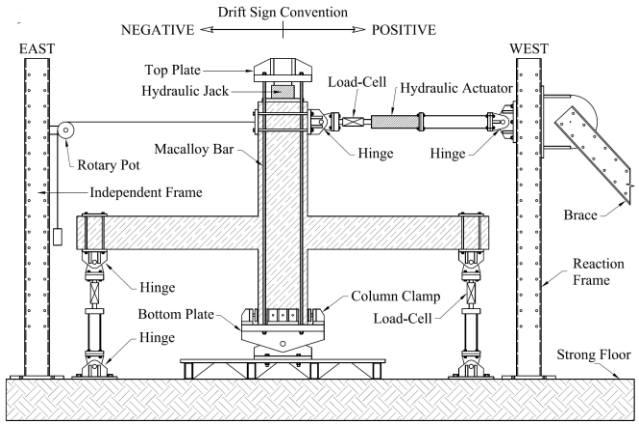

Figure 4: Details of the test setup for cyclic testing of BCJs.

The beams had four grade 300 MPa longitudinal deformed bars (two each of diameter 20 and 25 mm) at the top and bottom with four legs of R8 stirrups spaced at 90 mm c/c in the plastic hinge zone and 200 mm c/c elsewhere. On the other hand, the column had fourteen 20 mm diameter grade 300 MPa deformed longitudinal bars distributed around the perimeter with four legs of R10 grade 300 MPa stirrups spaced at 80 and 110 mm c/c in the plastic hinge zone and elsewhere, respectively. Similarly, the joint had five layers of equally spaced shear reinforcement each comprising of two HR10 and two HR12 legs (both of a higher yield strength of 500 MPa in contrast to the beam and column stirrups which had yield strength of 300 MPa); except for the specimen BCJ3 whose joint shear reinforcement comprised of four R10 legs of 300 MPa yield strength.

DIANA provides a wide variety of elements including but not limited to the truss, beam, plane stress, plane strain, axisymmetric, plate bending, flat shell, curved shell, solid, and interface elements. Due to the geometry of BCJ specimens and test setup as well as the loading direction, it is not necessary to use three-dimensional (solid) elements. Selection of solid elements for such analysis will only increase the computation effort and time required for the analysis without adding any significant value to the final outcome. Therefore, the finite element modelling was decided to consist of two-dimensional (2D) elements. The applicable 2D elements which could be employed in the FE model were channelled down to the plane stress, plate bending, flat shell, and curved shell elements (Figure 5). In the plate bending elements (Figure 5b), the direction of load should be perpendicular to the plane of the element; which is not the case in the BCJ specimens and the tests being simulated. Therefore, the 2D plate bending elements are ruled out. In DIANA, the embedded reinforcement option cannot be used in the flat shell elements (Figure 5c); which rules out the use of these elements. However, when using the curved shell elements (Figure 5d), there is an option for flat surfaces which is equivalent to the flat shell elements in which the embedded reinforcements may be used.

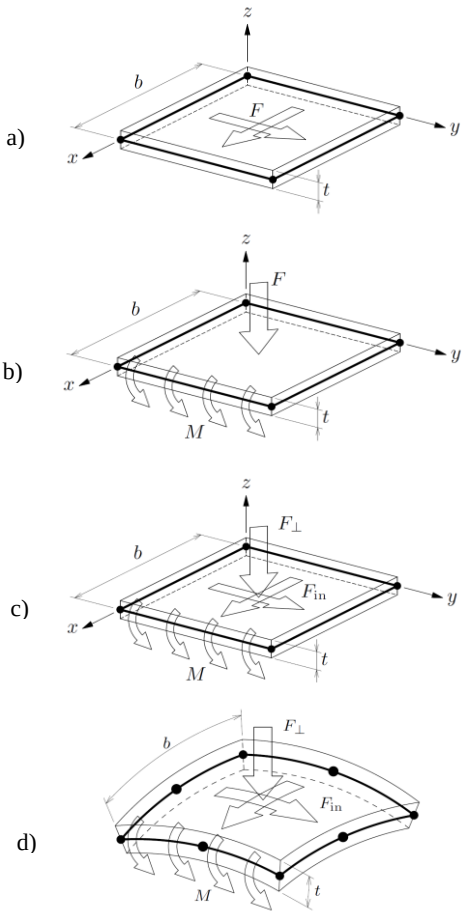

Figure 5: a) Plane stress, b) plate bending, c) flat shell, and d) curved shell elements available in DIANA.

If the plane stress elements (Figure 5a) are chosen, all of the reinforcement which is otherwise distributed along the thickness (340 mm) of the BCJs should be lumped into one plane. Although the computational effort and analysis time would decrease, this assumption unnecessarily reduces the accuracy of the generated FE model. This is important when different diameter bars of various yielding points are utilized along the thickness of the specimen; which was the case for the BCJs to be simulated in this study. By employing curved shell elements, the location of reinforcement (longitudinal and transverse) along the thickness of BCJs can be better represented and different diameter bars can easily be modelled. In addition, different material properties can be defined by incorporating different layers along the thickness and the out-of-plane deformations may be accounted for should any asymmetric or out-of-plane loadings be present in the model. Therefore, 2D curved-shell elements available in DIANA were used to model the 2D parts of the model (joint region, beam, column, linear concrete, and steel plates).

In generating the FE model, attention was paid to replicate different parts of the actual experiment in such a way that a balance of accuracy and simplicity in modelling was achieved. Steel plates of linear material properties and very high stiffness were used at the top and bottom of the column as well as the tip of the beams. Linear high stiffness truss elements of 300 mm diameter circular steel cross section were employed to connect the beam ends to their supports as in the experiments. The column and beam supports were all pinned and the column was

also supported laterally in the 'z' direction (perpendicular to the BCJ plane) to increase the stability of the FE model against the out-of-plane deformations of the curved shell elements. The axial load was applied through four unbonded pre-stressed steel tendons (35 mm diameter) connected to the top and bottom steel plates of the column. Note that the thickness of the 2D curved shell elements in 'z' direction was 340 mm; equal to the actual thickness of the specimens. Both the longitudinal and transverse reinforcement were modelled in their actual locations without compromising their distribution in 'z' direction (over the thickness). The joint region and the plastic hinge zone of the beam had a finer mesh, but a coarser mesh was used for the remaining parts. Figure 6 shows the details of the FE discretization described above.

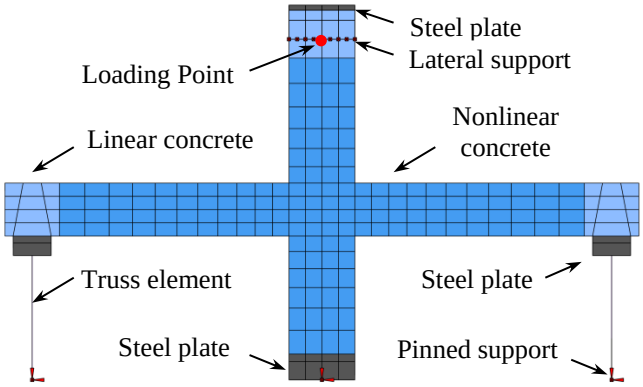

Figure 6: Different parts of the finite element model.

NONLINEAR FINITE ELEMENT ANALYSIS

The solution to a nonlinear analysis involves selecting an appropriate iterative procedure. DIANA offers four different iterative procedures; namely Newton-Raphson, Quasi-Newton, Linear Stiffness, and Constant Stiffness. The Quasi-Newton (otherwise known as Secant) method was chosen based on its capability in maintaining a stable analysis. When nonlinearities like cracking in RC structures occur in a model, the ordinary iteration process may have problem in converging. This is when applying a "line search" algorithm would be beneficial in keeping the iterative procedure stable and avoiding divergence. The line search method was employed in the analyses whenever divergence occurred.

The analysis involved two main stages: the application of axial load and lateral displacement cycles consecutively. As the axial and lateral loads were applied in the form of force and displacement controlled procedures, respectively; an "Energy Norm" of 0.0025 was used to control the convergence at each loading step for both loading types. The maximum number of iterations was set to 1000; however most of the loading steps converged within 30 iterations with a few exceptions.

The axial load was applied in ten equal loading steps to ensure that the stability of the analysis was maintained. The displacement controlled lateral loading protocol used in the laboratory was adopted, adjusted and applied to the top of the column. The displacement increment at each loading step was limited to 1 mm so that equilibrium could be achieved quickly and divergence was avoided. Also, to avoid problems associated with stress concentration around the point load/reactions, linear properties with high stiffness were assigned to the elements in the regions near the loading point and also near the beam supports. Mesh sensitivity analysis was also performed [31] in order to determine the most suitable mesh size so that a balance between computational effort and accuracy is achieved.

Pushover Analysis

Before applying the cyclic loading to the model, a pushover analysis was performed in order to check that the overall features of the response (such as the initial stiffness, yield point and peak load of each cycle) were comparable to that of the experiment. Figure 7 shows the load vs. displacement results of the FE pushover analysis of the joint against the experimental result. As it can be seen, the overall trend of the pushover curve follows the backbone of the experimental cyclic response. The yielding and post-yielding loads given by the FEA were higher compared to the experiment. However, such difference can occur between monotonic and cyclic responses, and one needs to conduct a cyclic FEA (presented in the following sections) to confirm if there is indeed a significant mismatch.

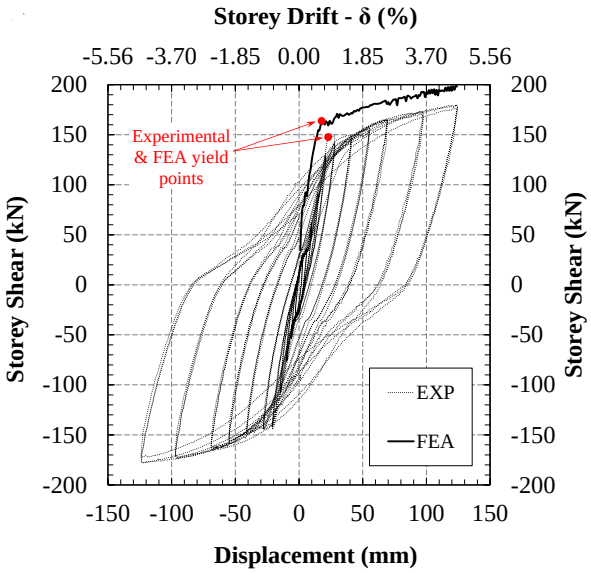

Figure 7: Comparison of the response envelope of the modelled BCJ predicted by pushover analysis with the cyclic experimental loops.

The initial stiffness of the FE model also seems to be slightly higher than the experimental stiffness. Due to the location of the bolts on the strong floor, the pin support at the base of the column had to be connected to the strong floor through a stiffened steel base (Figure 8a). As the steel base was about 200 mm high off the ground, suitable length bolts were used to fix it to the strong floor. As a result, slight movement was observed at the steel base when the column top was at its peak displacement. This displacement was not measured during the test; but an attempt was made to minimize it using a bracing at the base. This slackness may have been the reason for the higher stiffness in the FE model compared to that of the experiment. Due to the nature of the movement, it could be modelled using a linear spring quite reasonably (Figure 8b). To check its effect, another pushover analysis was performed after adding a linear spring along the 'X' direction at the column support. The overall movement of the base was measured at the maximum force/displacement of the column top, which was used to calibrate the spring stiffness to 17,500 N/mm. The results of the two cases are compared in Figure 8c.

As can be seen in the figure, the initial stiffness reduces without noticeably changing any other properties of the curve when the linear spring is added. It is clear from Figure 8c that the addition of spring provides a closer prediction of the experimental backbone curve; however, this also adds to the complexity of the model, which in turn makes it difficult to achieve convergence in the cyclic analysis. Nonetheless, the analyses reported hereafter were conducted with the linear spring added

at the column base (unless specified otherwise) to ensure the model better represents the actual conditions of the test setup.

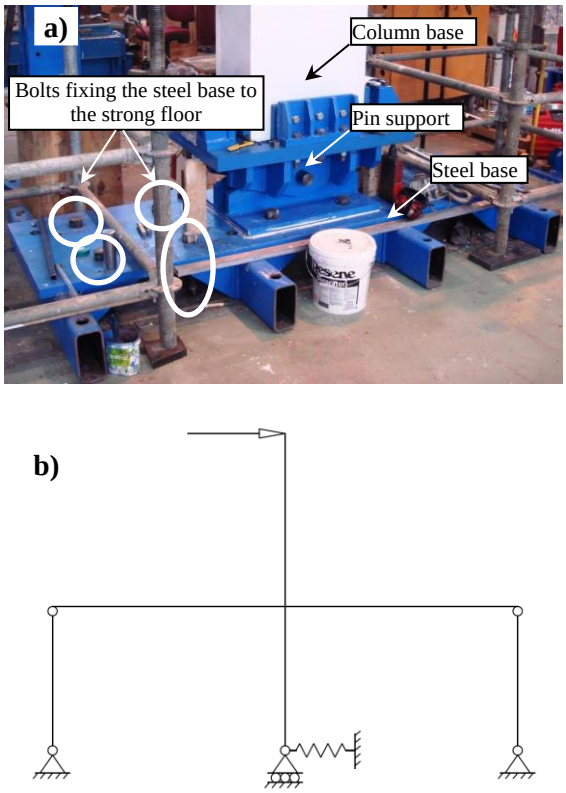

Figure 8: (a) Arrangement of the test setup at the column base; (b) schematic view of the spring support at the column base; and (c) pushover responses predicted with the spring added at the column base.

Cyclic Analysis

The cyclic responses measured in the experiment and predicted by the FEA are compared in Figure 9. Note that as opposed to the experiment where each loading cycle was repeated three times, only one cycle was applied for each drift in the FEA. Although this was done to reduce the required time for analysis, no significant difference was observed between the results of the three and one cycle repetitions.

As can be seen in Figure 9, after yielding the strength degradation is more pronounced in the cyclic analysis compared to that in the pushover analysis; which is due to the deleterious effects of cyclic loading on the material properties. In fact, the peak lateral forces achieved in the experiment were comparable to the peak forces obtained from the cyclic FEA. Even the loading and unloading stiffness were predicted with a reasonable accuracy. The FE response showed lesser pinching compared to the experiment; especially in the larger displacement cycles (2.5%, 3.5% and 4.5% drift ratios). The underestimation of pinching in the FE results comes mainly from the steel constitutive model, and it is believed that once the effect of buckling is incorporated in the steel constitutive model in DIANA, the FE result should be able to capture pinching better.

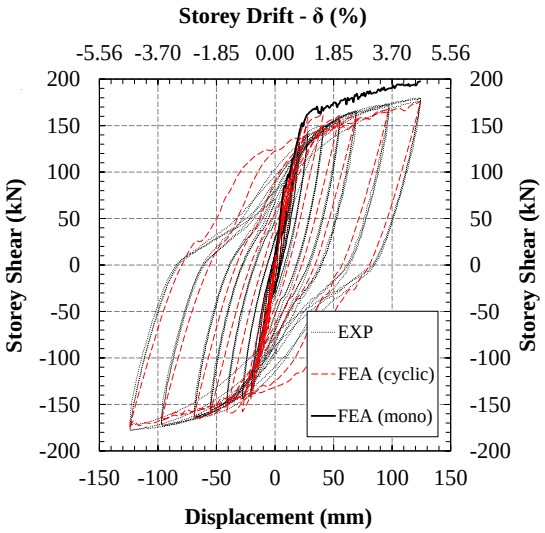

Figure 9: FEA vs. experimental results of BCJ1 with spring column base.

Other seismically important response measures such as damping, peak-to-peak secant stiffness, contribution of concrete and steel in joint shear resistance, joint shear deformation, and elongation of the beam plastic hinge zone were also compared between the experiment and FEA (Figure 10). As shown in the figure, there is a close agreement between the experimental and FEA results for most of the reported parameters. It is important noting that the joint shear stress does not directly correspond to the beam or column shear forces; rather it comes indirectly from the transformation of beam bending at the face of the column to a force couple in the beam bars and then transferred into the joint. Therefore, such accuracy in predicting the joint shear deformation can only result from a combination of close reproduction of the experimental conditions and the use of versatile and reliable material models in the numerical simulation and analysis.

It is obvious from Figure 10e that the FE model could predict elongation in the plastic hinge zone, however only about half of the actual elongation measured in the test was captured by the FEA. Note that in the experiment, elongation measurements were performed only up to the end of the 3.5% drift cycles after which the potentiometers had to be removed in order to avoid being damaged; this was obviously not the case in the FEA. At the end of the 3.5% drift, the FEA predicted only about 13 mm elongation as opposed to 30 mm measured in the experiment. Even after repeating the cycles three times for each drift amplitude (same as in the test), the predicted elongation did not increase to the same extent as in the experiment. This is because the material strains increased only marginally during the repeated cycles of equal drift, and deterioration of the materials during repeated cycles of the same strain amplitude was not incorporated in the material models adopted in the FEA. In order to facilitate direct comparison between the predicted (i.e. FEA) and measured (i.e. experimental) elongations, the experimental elongation results were modified in such a way that the effect of the two repeated cycles on beam elongation was omitted and the modified results were compared to the

elongation predicted by the FEA (Figure 10f). It is clear from Figure 10f that once the two additional drift cycles were excluded from the recorded elongation data, the FEA and experimental result showed a considerably closer agreement. At drift ratio of 3.5%, the experiment and FEA showed an elongation of about 4% and 3% of the beam depth, respectively. This is comparable to elongation reported in literature based on cyclic tests and numerical analyses of conventionally vibrated RC beams and frames [32-36].

In order to go even deeper into the details, strain development in the joint shear stirrups were extracted and compared with the readings of strain gauges installed on the surface of the joint shear reinforcement in the test (Figure 11). The FE results for

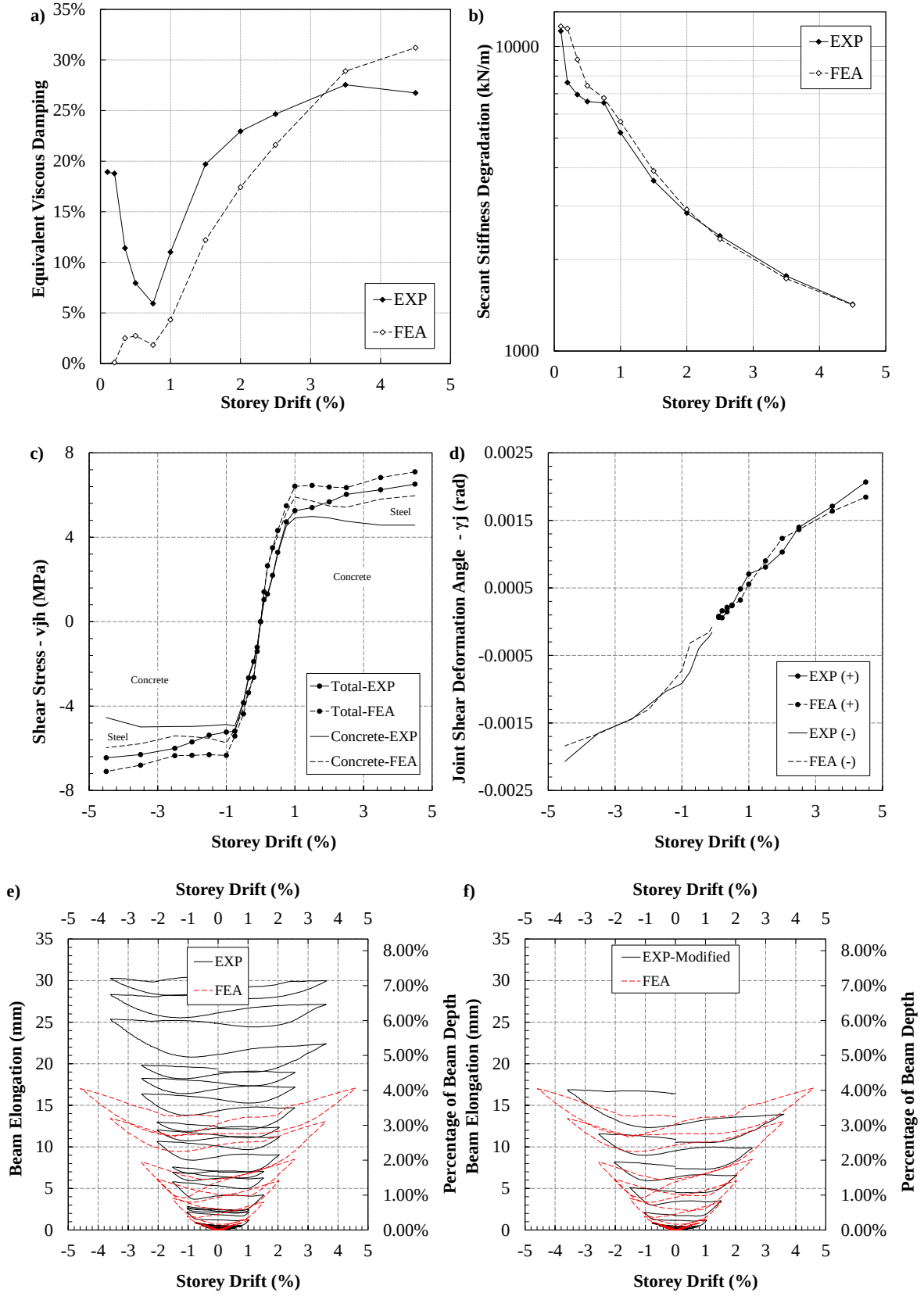

Figure 10: Comparison of experiment and FEA of other seismically important features.

the strain in joint shear reinforcement at different drift ratios were similar to the strain gauge readings in the test. Agreeing with the experimental observation, the analytically predicted strains also remained well below the half-yield line indicated by the dashed line in Figure 11. Note that as the joint and column stirrups had slightly different strengths, the half-yield line is not straight. The experimental strain profiles observed during the negative peaks (Figure 11c) were predicted more accurately by the FEA (Figure 11d) compared to the ones at the positive peaks (Figures 11a & b). Nevertheless, considering that the strain gauge readings are expected to vary significantly as they are sensitive to local conditions that are difficult to control in the test and impossible to account for in analysis, the overall prediction of strain profiles in the joint stirrups were considered acceptable.

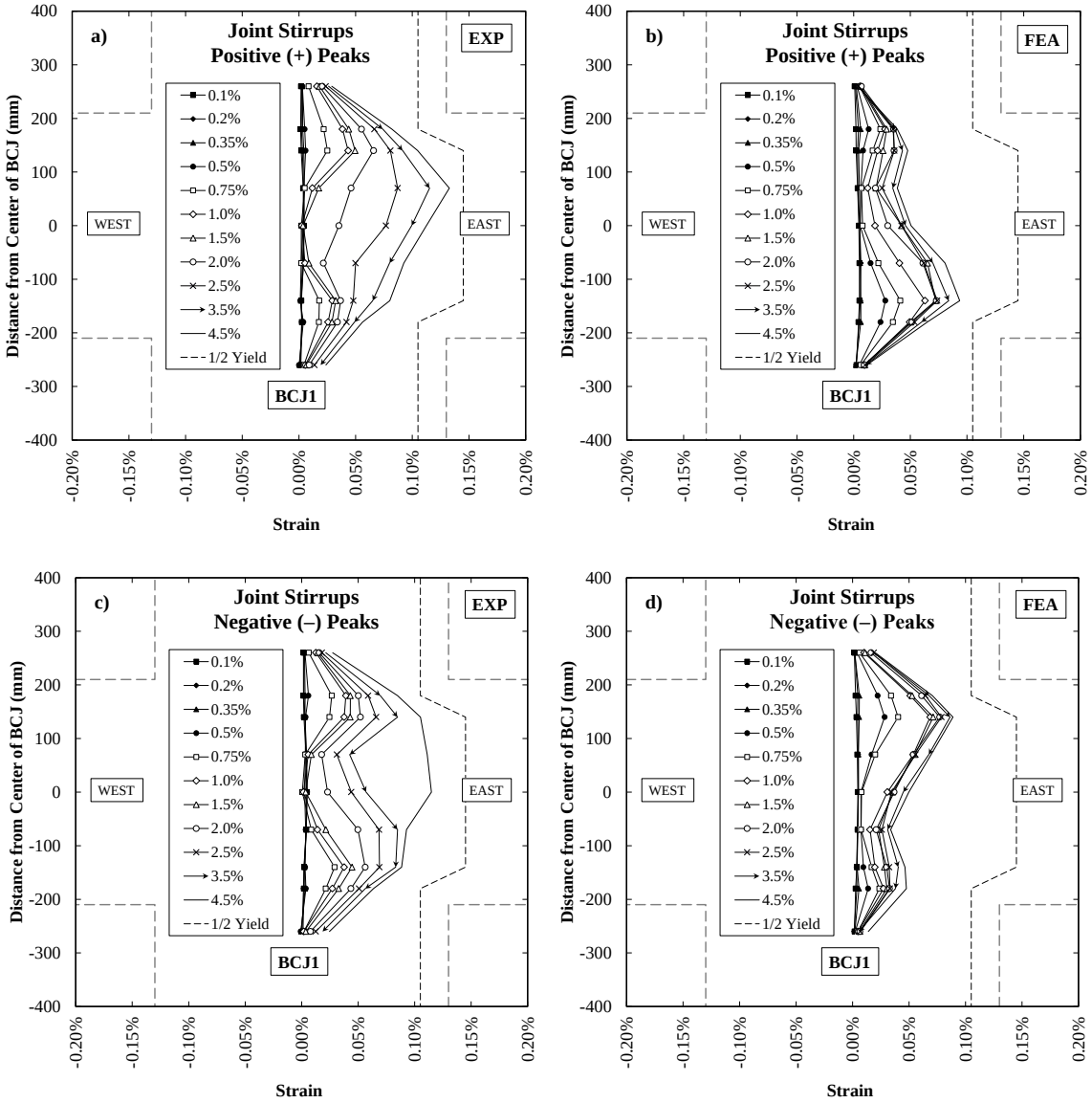

Figure 11: Strain profiles in the joint shear stirrups at the positive and negative peaks of different drift cycles obtained from experimental measurements and numerical prediction.

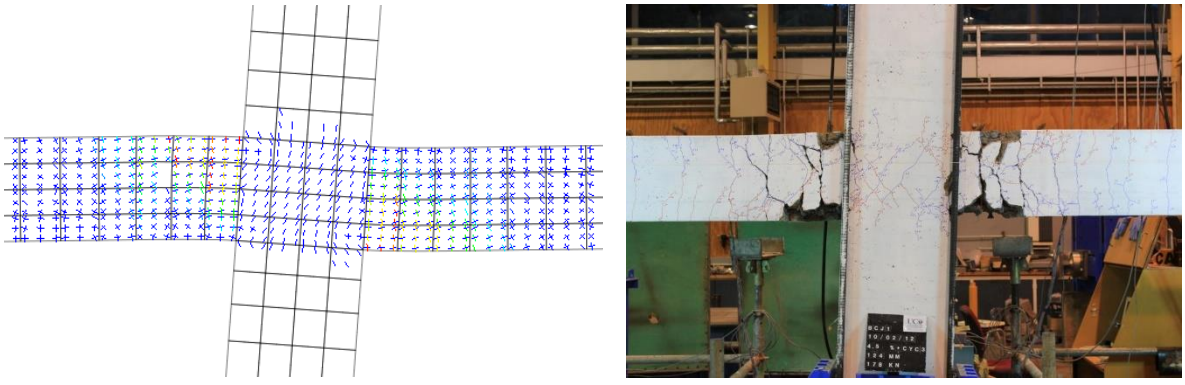

Figure 12: Comparison of crack patterns between the experiment and FEA analysis.

The crack patterns predicted by the FEA are compared to those from the experiment in Figure 12, which shows that the FE model could reasonably predict the location and direction of the cracks. Note that because of the rotating crack model used in the analysis, cracks which appeared in the previous cycle would disappear on load reversal which is equivalent to crack closure in the experiment.

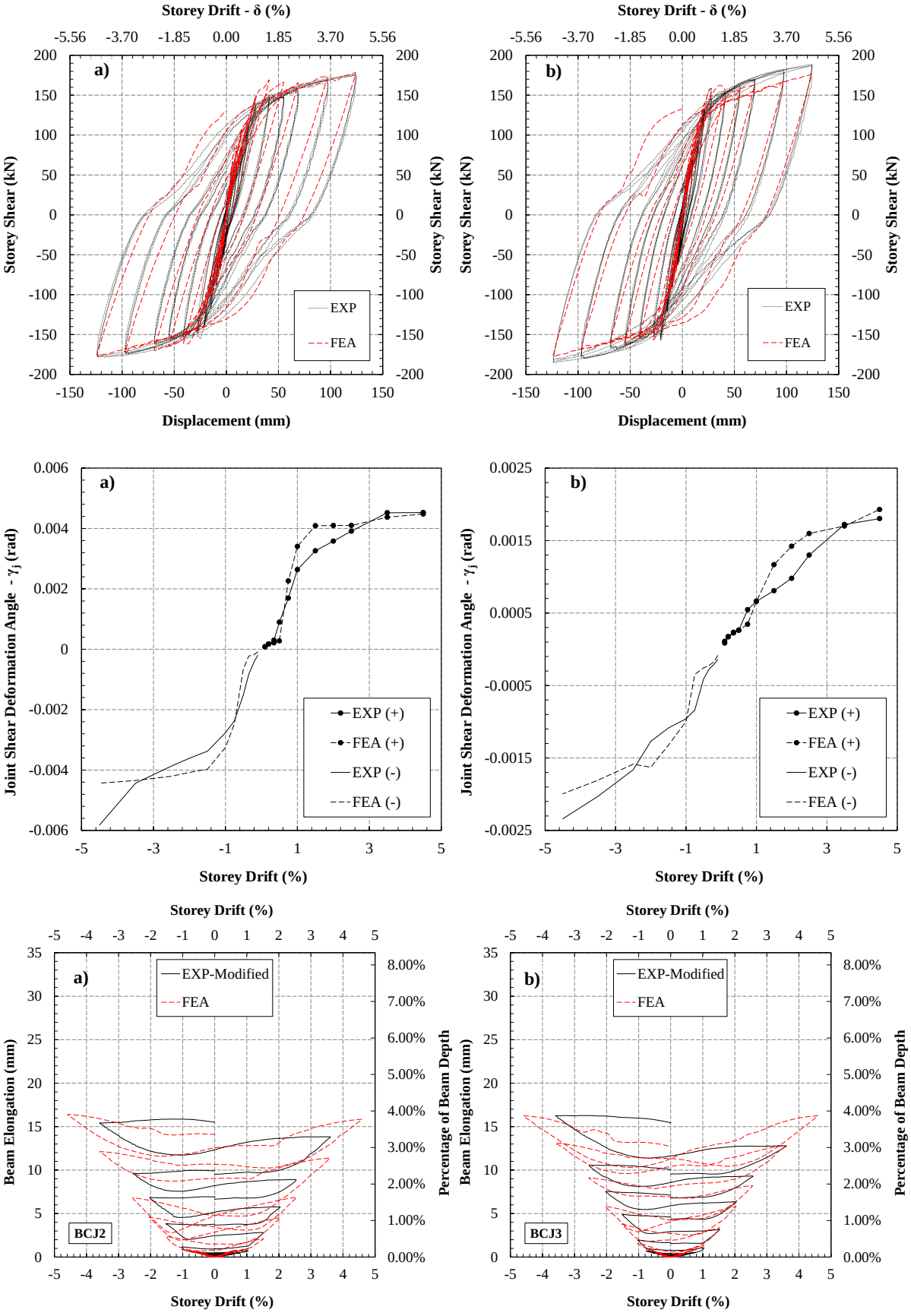

Figure 13: Comparison of experimental and FEA results for (a) BCJ2 and (b) BCJ3.

VERIFICATION OF FEA FOR OTHER SPECIMENS

In order to more extensively verify the validity of the FE modelling and predictions, two more tested BCJ specimens were modelled and analysed (with springs at the column end to simulate the support movement in the tests). The first specimen, named BCJ2 has a smaller axial load (1%) and the other, named BCJ3, is with less amount of joint shear reinforcement (almost half of BCJ1 and BCJ2); details of these specimens can be found elsewhere [30,31]. The experimental and analytical results of these two specimens are shown in Figure 13. As it can be seen, in both specimens the FEA could predict (with reasonable accuracy) the cyclic hysteretic response, the joint deformation, and the beam elongations. Although not presented here due to space limitations, other seismically important features (such as strength/stiffness degradation, increase in equivalent viscous damping, joint shear response, and strain profiles) derived from FEA were also compared to those of experimental results and close agreement was observed between the two. Further details on these comparisons can be found in the first author's PhD thesis [31].

CONCLUSIONS

In this study, the finite element analysis (FEA) program "DIANA" was used to model seismic performance of high-strength self-compacting concrete (HSSCC) beam-column joints (BCJs) under cyclic loading. BCJ subassemblies tested by the authors were modelled and nonlinear monotonic and cyclic analyses were performed on the modelled specimens and validated by comparing with the test results.

Pushover analyses were conducted first to get the basic idea of the pros and cons of the model developed, to decide on the suitability of the adopted material models, and to fine-tune the model if needed. The preliminary investigation suggested that the most appropriate approach would be to use 2D curved shell elements together with reinforcing bar elements embedded in their actual locations across the thickness. The predictions were found to be reasonable when the material constitutive models were based on total strain rotating crack model (for concrete) and the Menegotto-Pinto model combined with an experimentally calibrated bilinear envelope (for reinforcing bars). Further details on these comparisons can be found in the first author's PhD Thesis [31].

As expected, the pushover analysis slightly overestimated the experimental hysteresis envelope, but the envelope obtained from the cyclic analysis was closer to the test results; thereby suggesting that the material models were able to reasonably capture the cyclic deterioration. While pinching was slightly underestimated as bar buckling was not accounted for in the reinforcement constitutive model, the cyclic hysteresis loops captured by FEA in general showed a very close agreement to that of the actual test.

Other seismically important features such as the damping, peak-to-peak secant stiffness, contribution of concrete and steel in joint shear resistance, joint shear deformations, and elongation of the beam plastic hinge zone were also compared between the experiment and FEA. It was found that except for the elongation of the beam plastic hinge, other response parameters predicted by the FEA closely agreed with the experimental results. After accounting for the increase in elongation due to repeated displacement cycles, an acceptable agreement was observed between the experimental and analytical elongation results as well.

To prove the versatility of the developed FEA approach, two more experimentally tested BCJ specimens (with different axial load and joint shear reinforcement) were also modelled and analysed. Reasonable agreement was observed between the FEA and experimental results for both specimens. As the finite element analysis program DIANA with the selected elements and material models was found to be capable of satisfactorily dealing with the complexities involved in modelling and analysing HSSCC beam-column joints, it can be relied on to predict (with acceptable accuracy) seismic behaviour of RC frames comprising HSSCC joints.

ACKNOWLEDGMENTS

The authors would like to acknowledge the funding provided for the project by the Earthquake Commission (EQC) New Zealand.

REFERENCES

1 Deaton JB (2013). "*Nonlinear Finite Element Analysis of Reinforced Concrete Exterior Beam-Column Joints with Non-seismic Detailing*". PhD Thesis, Georgia Institute of Technology, USA.

2 Li B, Tran CTN and Pan TC (2009). "Experimental and numerical investigations on the seismic behavior of lightly reinforced concrete beam-column joints". *ASCE Journal of Structural Engineering*, **135**(9): 1007-1018.

3 Sharma A, Genesio G, Reddy GR and Eligehausen R (2009). "Nonlinear dynamic analysis using microplane model for concrete and bond slip model for prediction of behavior of non-seismically detailed RCC beam-column joints". *Journal of Structural Engineering (Madras)*, **36**(4): 250-257.

4 TNO DIANA BV (2012). "*DIANA Manual Release 9.4.4*". Delft, The Netherlands.

5 Li B and Cao Thanh Ngoc T (2009). "Seismic behavior of reinforced concrete beam-column joints with vertically distributed reinforcement". *ACI Structural Journal*, **106**(6): 790-799.

6 Dashti F, Dhakal RP and Pampanin S (2017). "Numerical modeling of rectangular reinforced concrete structural walls". *ASCE Journal of Structural Engineering*, **143**(6):04017031.

7 Vecchio FJ and Collins MP (1986). "Modified compression field theory for reinforced concrete elements subjected to shear". *Journal of the American Concrete Institute*, **83**(2): 219-231.

8 Litton RW (1974). "*A Contribution to the Analysis of Concrete Structures under Cyclic Loading*". University of California, Berkeley, CA.

9 Selby RG, Vecchio FJ and Collins MP (1996). "Analysis of reinforced concrete members subject to shear and axial compression". *ACI Structural Journal*, **93**(3): 306-315.

10 Selby RG and Vecchio FJ (1997). "A constitutive model for analysis of reinforced concrete solids". *Canadian Journal of Civil Engineering*, **24**(3): 460-470.

11 Thorenfeldt E, Tomaszewicz A and Jensen JJ (1987). "Mechanical properties of high-strength concrete and applications in design". *Symposium on Utilization of High-Strength Concrete*. Stavanger, Norway.

12 Hordijk D (1991). "*Local Approach to Fatigue of Concrete*". PhD Thesis, Delft University of Technology, The Netherlands.

13 Menegotto M and Pinto E (1973). "Method of analysis for cyclically loaded reinforced concrete plane frames including changes in geometry and non-elastic behaviour of elements under combined normal force and bending".

IABSE Symposium on the Resistance and Ultimate Deformability of Structures Acted on by Well-Defined Repeated Loads. Lisbon, Portugal.

14 Cofie N and Krawinkler H (1985). "Uniaxial cyclic stress-strain behavior of structural steel". *ASCE Journal of Engineering Mechanics*, **111**(9): 1105-1120.

15 Dodd LL and Restrepo-Posada JI (1995). "Model for predicting cyclic behavior of reinforcing steel". *ASCE Journal of Structural Engineering*, **121**(3): 433-444.

16 Balan TA, Filippou FC and Popov EP (1998). "Hysteretic model of ordinary and high-strength reinforcing steel". *ASCE Journal of Structural Engineering*, **124**(3): 288-297.

17 Hoehler MS and Stanton JF (2006). "Simple phenomenological model for reinforcing steel under arbitrary load". *ASCE Journal of Structural Engineering*, **132**(7): 1061-1069.

18 Heo Y, Zhang G, Kunnath S and Xiao Y (2009). "Modeling cyclic behavior of reinforcing steel: Relevance in seismic response analysis of reinforced concrete structures". *Key Engineering Materials*, **400-402**: 301-309.

19 Monti G and Nuti C (1992). "Nonlinear cyclic behavior of reinforcing bars including buckling". *ASCE Journal of Structural Engineering*, **118**(12): 3268-3284.

20 Gomes A and Appleton J (1997). "Nonlinear cyclic stress-strain relationship of reinforcing bars including buckling". *Engineering Structures*, **19**(10): 822-826.

21 Rodriguez ME, Botero JC and Villa J (1999). "Cyclic stress-strain behavior of reinforcing steel including effect of buckling". *ASCE Journal of Structural Engineering*, **125**(6): 605-612.

22 Dhakal RP and Maekawa K (2002). "Modeling for postyield buckling of reinforcement". *ASCE Journal of Structural Engineering*, **128**(9): 1139-1147.

23 Dhakal RP and Maekawa K (2002). "Reinforcement stability and fracture of cover concrete in RC members". *ASCE Journal of Structural Engineering*, **128**(10): 1253-1262

24 Dhakal RP and Maekawa K (2002). "Path-dependent cyclic stress-strain relationship of reinforcing bar including buckling". *Engineering Structures*, **24**(11): 1383-1396.

25 Fleury F, Reynouard JM and Merabet O (1999). "Finite element implementation of a steel-concrete bond law for nonlinear analysis of beam-column joints subjected to earthquake type loading". *Structural Engineering and Mechanics*, **7**(1): 35-52.

26 Sasmal S, Novak B and Ramanjaneyulu K (2010). "Numerical analysis of under-designed reinforced concrete beam-column joints under cyclic loading". *Computers and Concrete*, **7**(3): 203-220.

27 Orakcal K, Massone LM and Wallace JW (2006). "*Analytical Modeling of Reinforced Concrete Walls for Predicting Flexural and Coupled-Shear-Flexural Responses*". Pacific Earthquake Engineering Research Center, University of Californina, Los Angeles, CA.

28 Standards New Zealand (2006). "*NZS3101 Concrete Structures Standard Parts 1 & 2: The Design of Concrete Structures and Commentary*". Standards New Zealand, Wellington, NZ.

29 Soleymani Ashtiani M, Scott AN and Dhakal RP (2013). "Mechanical and fresh properties of high-strength self-compacting concrete containing class C fly ash". *Construction and Building Materials*, **47**: 1217-1224.

30 Soleymani Ashtiani M, Dhakal RP and Scott AN (2014). "Seismic performance of high-strength self-compacting concrete in reinforced concrete beam-column joints". *ASCE Journal of Structural Engineering*, 140(5): 04014002.

31 Soleymani Ashtiani M (2013). "*Seismic Performance of High-Strength Self-Compacting Concrete in Reinforced Concrete Structures*". PhD Thesis, Department of Civil and Natural Resources Engineering, University of Canterbury, Christchurch.

32 Walker AF and Dhakal RP (2009). "Assessment of material strain limits for defining plastic regions in concrete structures." *Bulletin of the New Zealand Society of Earthquake Engineering*, **42**(2): 86-95.

33 Peng BHH, Dhakal RP, Fenwick R, Carr A and Bull D (2011). "Elongation of plastic hinges in ductile RC members: Model development". *Journal of Advanced Concrete Technology*, 9(3):. 315-326.

34 Peng BHH, Dhakal RP, Fenwick R, Carr A and Bull D (2011). "Elongation of plastic hinges in ductile RC members: Model verification". *Journal of Advanced Concrete Technology*, **9**(3): 327-338.

35 Peng BHH, Dhakal RP, Fenwick R, Carr A and Bull D (2013). "Multi-spring hinge element for reinforced concrete frame analysis". *ASCE Journal of Structural Engineering*, **139**(4): 595-606.

36 Dhakal RP, Peng BHH, Fenwick R, Carr A and Bull D (2014). "Cyclic loading test of a RC frame with precast-prestressed flooring system". *ACI Structural Journal*, **111**(4): 777-788.